ATMOSPHERIC SCIENCE

Water isotope ratios reflect convection intensity rather than rain type proportions in the pantropics

Wusheng Yu[1]*†, Rong Guo[1,2]†, Lonnie G. Thompson[3], Jingyi Zhang[1], Stephen Lewis[4], Zhaowei Jing[5], Junmei He[1,6], Yaoming Ma[1,2,7], Baiqing Xu[1], Guangjian Wu[1], Xu Zhou[1], Wenjun Tang[1], Qiaoyi Wang[1,2], Pengjie Ren[1,2], Zhuanxia Zhang[1,2], Dongmei Qu[1]

Against the traditional view, a recently published theory argued that isotope ratios are higher in convective precipitation but lower in stratiform precipitation and proposed that isotope ratios reflect rain type proportions. This theory has been widely cited despite some early reservations. Whether the theory represents a faithful reflection of signals of water isotope ratios remains unclear. Here, we reassess its validity from different timescales and broader observations from the pantropics. Unexpectedly, our findings contradict the theory on daily, monthly, and even annual timescales. Pantropical precipitation isotope ratios remain strongly correlated to convection intensity but are independent of rain type proportions because stratiform precipitation isotope ratios cover a large range of values. We find that the theory has many serious weaknesses related to preferential data selection and suggest that new theories need to be validated at more locations on different timescales before gaining widespread acceptance.

INTRODUCTION

As early as 1964, Dansgaard carried out the pioneering work on the precipitation "amount effect" whereby a negative correlation between stable isotope ratios ($\delta^{18}O$) in precipitation and the corresponding precipitation amount was documented for tropical regions (*1*). This finding provided the fundamental basis for paleohydroclimate reconstructions using stable isotope records preserved in ice cores, speleothems, and tree rings obtained from the low latitudes. However, some recent studies have reported that the negative correlation between $\delta^{18}O$ and local precipitation amount is not significant (*2*–*8*) or that even a weak positive correlation has been noted at some locations (*9*, *10*). On the basis of these studies, the validity of the amount effect has been questioned (*11*–*16*). Should this amount effect relationship be disproven, several valuable paleoclimate records from the tropics would need urgent reappraisal.

An alternative theory has recently been proposed by Aggarwal *et al.* (*17*), which suggests that $\delta^{18}O$ variability in the tropical and mid-latitude regions is linked to rain types (hereafter called "stratiform fraction" theory, abbreviated as SF theory) rather than amount effect. On the basis of data from 28 tropical sites and 2 mid-latitude sites, they found that the relationship between the multiyear mean monthly $\delta^{18}O$ and precipitation amount was weak, while the $\delta^{18}O$ was strongly and negatively correlated with stratiform fraction precipitation [the coefficient of determination (R^2) = 0.59] (*17*). Hence, it was postulated that water isotope ratios in tropical and mid-latitude precipitation reflect rain type proportions with relatively lower $\delta^{18}O$ within stratiform precipitation and higher $\delta^{18}O$ in convective precipitation (*17*). They further postulated that stable isotope records in proxy archives (such as ice cores and speleothems) from the low latitudes need reinterpretation to reflect the proportions of convective and stratiform precipitation, which may or may not coincide with drier or wetter conditions (*17*). Although this SF theory was initially met with some skepticism (*8*, *18*–*20*), it has gradually gained wider acceptance (*21*–*26*).

A number of subsequent studies now attribute $\delta^{18}O$ depletion in tropical precipitation to a dominance of stratiform precipitation (*22*–*25*). Some studies have even argued that groundwater isotope ratios also reflect the bulk proportions of convective/stratiform precipitation (*27*). Since the advent of the SF theory, more studies have used rain types (or lower stratiform precipitation isotope ratios or higher convective precipitation isotope ratios) to reconcile apparent contradictions within paleoclimate reconstructions (*28*–*30*). However, it is not clear if the SF theory provides a faithful reflection of the true water isotopic signal in tropical precipitation and the foundations for the theory have not received rigorous examination. There is a clear need to examine the basis of the SF theory so that the drivers of $\delta^{18}O$ in tropical precipitation are understood and to ensure that paleoclimate proxy records can be confidently interpreted.

In this study, we replicated the work underlying the SF theory and also explored the relationships between $\delta^{18}O$ and the stratiform fraction at more locations on different timescales (daily, monthly, and annual). Here, we focused on the observations from the pantropics (defined as the regions of 35°N to 35°S in this study for the convenience of narrative, although some locations seem relatively far outside the tropics) because the precipitation amount effect was found in the regions (*1*). Contrary to the SF theory, we found that precipitation isotope ratios in the pantropics are not related to rain types but rather are closely related to convection strength whether on daily, monthly, or even annual timescales. We conclude that water isotope ratios in the pantropics do not reflect rain type proportions, which discounts the SF theory.

[1]State Key Laboratory of Tibetan Plateau Earth System, Environment and Resources (TPESER), Institute of Tibetan Plateau Research, Chinese Academy of Sciences, Beijing 100101, China. [2]University of Chinese Academy of Sciences, Beijing 100049, China. [3]Byrd Polar and Climate Research Center, The Ohio State University, Columbus, OH 43210, USA. [4]Catchment to Reef Research Group, Centre for Tropical Water and Aquatic Ecosystem Research, James Cook University, Townsville, QLD 4811, Australia. [5]Laoshan Laboratory, Qingdao 266061, China. [6]Faculty of Geography, Yunnan Normal University, Kunming 650500, China. [7]College of Atmospheric Science, Lanzhou University, Lanzhou 730000, China.
*Corresponding author. Email: yuws@itpcas.ac.cn
†These authors contributed equally to this work.

RESULTS AND DISCUSSION

Stratiform fraction and water isotope ratios

We compiled published daily $\delta^{18}O$ data and the corresponding precipitation amount data from 38 sites in the pantropics during the period of 1998 to 2021 (Fig. 1, black crosses, and table S1). We also retrieved the corresponding daily stratiform fraction data from the Global Precipitation Measurement (GPM) 3GCSH Tropical Rainfall Measuring Mission (TRMM) (1998 to 2014) and GPM 3GCSH (2014 to 2021) and the daily outgoing longwave radiation (OLR) data (i.e., convection intensity) from ERA5 (the fifth generation ECMWF atmospheric reanalysis of the global climate) reanalysis (1998 to 2021) for these 38 sites. See Materials and Methods and Data and materials availability for details.

We examined the correlations between the daily $\delta^{18}O$ and stratiform fraction and OLR at 38 sites in the pantropics (Fig. 2, A and B). Unexpectedly, on the daily timescale, the relationship between $\delta^{18}O$ and the stratiform fraction in our study region was quite insignificant (R^2 is as low as 0.02). Thus, on the daily timescale, the $\delta^{18}O$ was independent of the stratiform fraction. Instead, the daily $\delta^{18}O$ was positively correlated with OLR ($R^2 = 0.14$). The result indicates that lower OLR values correspond to stronger convection activities and more depleted $\delta^{18}O$ values. Specific to the site locations, the negative correlation of the $\delta^{18}O$-stratiform fraction was only significant at 6 sites, while 16 sites displayed a positive correlation between $\delta^{18}O$ and the stratiform fraction (table S1). In contrast, $\delta^{18}O$ values were positively correlated with OLR at all sites, with 33 of the 38 sites having a significant positive correlation. Hence, the number of sites with a negative correlation between $\delta^{18}O$ and the stratiform fraction in the pantropics was far less than that with the positive correlation between $\delta^{18}O$ and OLR (table S1). The results on the daily timescale indicate that water isotope ratios in the pantropics are strongly affected by convection rather than the stratiform fraction.

We then attempted to replicate the study of the SF theory on the monthly timescale. We selected pantropical sites located in the 35°N to 35°S latitudinal range "with a minimum of four consecutive years of isotope data in the 1998 to 2014 period" as performed by the SF theory. On the basis of the criteria, however, we note that four sites in the study of the SF theory should be eliminated as the Jakarta and Manila sites were invalid (they are outside the relevant time frame; see Materials and Methods for details) and two mid-latitude sites of Vienna and Krakow are located beyond the specified latitudinal range for our study region. Hence, we retrieved the monthly $\delta^{18}O$ and the corresponding precipitation amount data from the remaining 26 valid sites (shown by green dots in Fig. 1) as well as from an additional 27 global network of isotopes in precipitation (GNIP) sites that meet the criteria (Fig. 1, yellow dots) (in total of 53 sites; table S2). We also retained the complete data for all months unlike the study of the SF theory, which excluded data where the multiyear average monthly precipitation was less than 50 mm (*17*). In addition, we retrieved monthly stratiform fraction data from TRMM 3H31 that has a higher spatial resolution of 0.5° grid cell and obtained monthly OLR data from ERA5 reanalysis with a spatial resolution of 0.25° × 0.25° and a temporal resolution of 1 hour for these 53 sites. See Materials and Methods and Data and materials availability for details.

Similar to the analysis on the daily time series data, there was a very weak negative correlation ($R^2 = 0.02$) between the monthly $\delta^{18}O$ and the stratiform fraction for all sites (Fig. 2C). By contrast, the linear correlation between monthly $\delta^{18}O$ and OLR is positive and very strong ($R^2 = 0.34$) (Fig. 2D). These findings suggest that the $\delta^{18}O$ values are strongly affected by convection with little influence from rain types. Specific to the site scale, moreover, the results were also very similar to the analysis from the daily timescale (table S2).

We further conducted similar analysis on the annual timescale (all sites and data are based on the monthly timescale) and still could not produce a robust negative linear relationship between $\delta^{18}O$ and the stratiform fraction ($R^2 = 0.08$). However, annual $\delta^{18}O$ remained significantly correlated with annual OLR ($R^2 = 0.45$) (Fig. 1, E and F).

More unexpectedly, a weak positive correlation between $\delta^{18}O$ and the stratiform fraction appears on both monthly and annual timescales when only the data where the stratiform fraction was greater than 60% were considered (fig. S1, A to C). However, a significant positive correlation between $\delta^{18}O$ and the corresponding OLR data also remains (fig. S1, D to F). It can be seen that, at more locations and on different timescales, the main factor governing the variation of the $\delta^{18}O$ in the pantropics is not rain types but the intensity of convection.

In short, all of the above results indicate that our findings oppose the SF theory. Here, we contend that the theory is not supported by the extensive databases compiled from the pantropics whether on daily, monthly, or even annual timescales. Although the $\delta^{18}O$ values

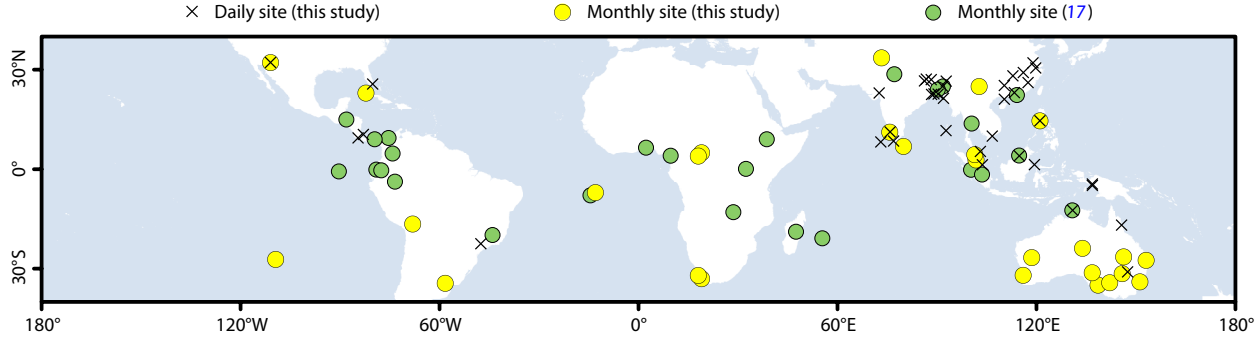

Fig. 1. Location of the 38 precipitation sampling sites on the daily timescale (black crosses) and 53 precipitation sampling sites on the monthly timescale. The 38 sites were selected from the published literature. On the monthly timescale, the 26 GNIP sites analyzed by (*17*) (green dots) as well as an additional 27 GNIP sites were also included in this study (yellow dots) (see table S2 for details).

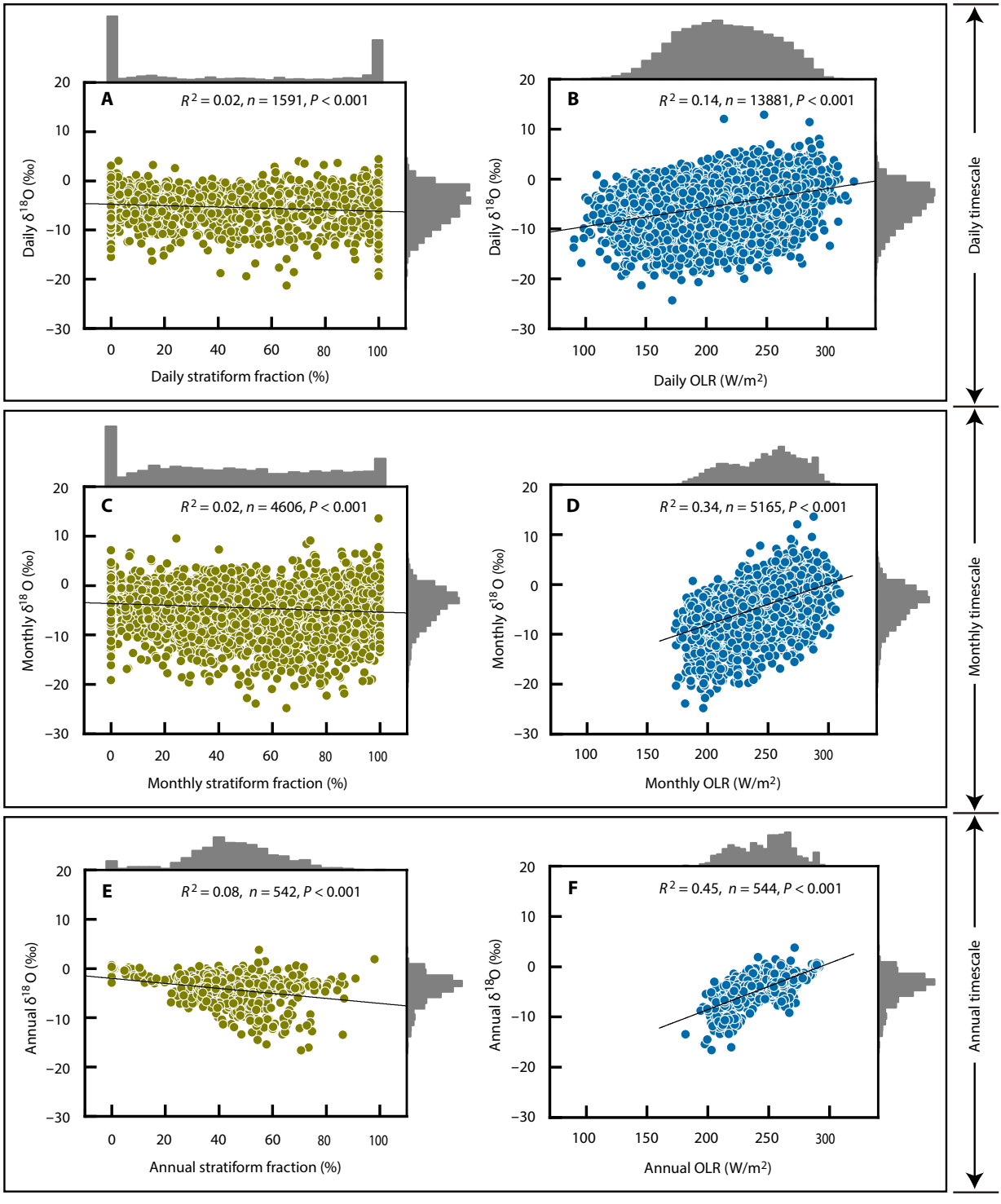

Fig. 2. Correlations between $\delta^{18}O$, stratiform fraction, and OLR in the pantropics on different timescales. (**A** and **B**) Daily timescale. (**C** and **D**) Monthly timescale. (**E** and **F**) Annual timescale. [(A), (C), and (E)] $\delta^{18}O$ and stratiform fraction. [(B), (D), and (F)] $\delta^{18}O$ and OLR (see Materials and Methods). The histogram illustrates the distribution of the datasets at 30 identical intervals.

are negatively correlated with the stratiform fraction at a few sites, the link may still be due to the intensity of convection, as we will now discuss further.

Exposing the weaknesses of the SF theory

On the basis of our findings, a question is raised on how the SF theory obtained the strong negative linear relationship between the two datasets. To investigate the dichotomy between the SF theory and our findings, we systematically analyzed the multiyear mean monthly data relationships across pantropical locations via a three-step process. These steps are (1) the replication of the original dataset from the study of the SF theory, (2) the inclusion of all available data from the original sites, and (3) the inclusion of all available site data from our study region.

Using the 26 valid sites of the SF theory and excluding the monthly data that contained precipitation of <50 mm, we find that a strong negative correlation between the stratiform fraction and $\delta^{18}O$ (R^2 = 0.32) does appear (Fig. 3A, step 1). However, if the complete dataset that contains all months are used, the strength of the negative correlation for the 26 sites reduces considerably ($R^2 = 0.16$) (Fig. 3B, step 2). In particular, when we include the 27 additional sites that also meet the SF theory criteria, we find that the strong negative linear relationship between the stratiform fraction and $\delta^{18}O$ collapses ($R^2 = 0.04$) (Fig. 3E, step 3). When the stratiform fraction is greater than 60%, the $\delta^{18}O$ also has a weak increasing trend with increasing stratiform fraction (fig. S2A). Through this step-by-step systematic analysis, we find that the reason why the stratiform fraction was strongly and negatively correlated with $\delta^{18}O$ in the study of the SF theory was due to the preferential selection of data within that analysis. This involved the exclusion of some monthly site data and apparently relevant datasets as well as the inclusion of invalid sites (see text S1, fig. S3, and tables S3 and S4 in the Supplementary Materials for details).

Expectedly, the correlations between the multiyear mean monthly $\delta^{18}O$ and OLR are notably stable when the same three-step process is applied (R^2 0.41, 0.44, and 0.41 for step 1, step 2, and step 3, respectively) (Fig. 3, B, D, and F). This finding indicates that, no matter what sites are chosen or how $\delta^{18}O$ data are selected for the given months, a strong positive linear correlation between $\delta^{18}O$ and OLR almost always occurs at pantropical locations. This result further demonstrates the key role of convection on $\delta^{18}O$ variability. In contrast, a strong negative correlation between $\delta^{18}O$ and the stratiform fraction can only be achieved by preferential selection of data and sites.

The correlation between $\delta^{18}O$ and the stratiform fraction at pantropical locations not only is less significant than the correlation between $\delta^{18}O$ and OLR but is also lower than the correlations between $\delta^{18}O$ and precipitation amount on different timescales (daily, monthly, and annual average monthly) (see fig. S4).

Some cases of stratiform precipitation with isotope enrichment

Precipitation in the pantropics is mostly composed of two types (convective and stratiform), and the annual mean dual-frequency precipitation radar area coverage for stratiform precipitation is larger than that for cold-topped convective precipitation (*31*). However, in the pantropics the zonally averaged echo-top height for cold-topped convective precipitation is higher than that for stratiform precipitation (*31*). Moreover, precipitation is dominated by convective precipitation (*31*) as organized (or mesoscale) convective systems are particularly strong in the pantropics [the annual stratiform precipitation fraction

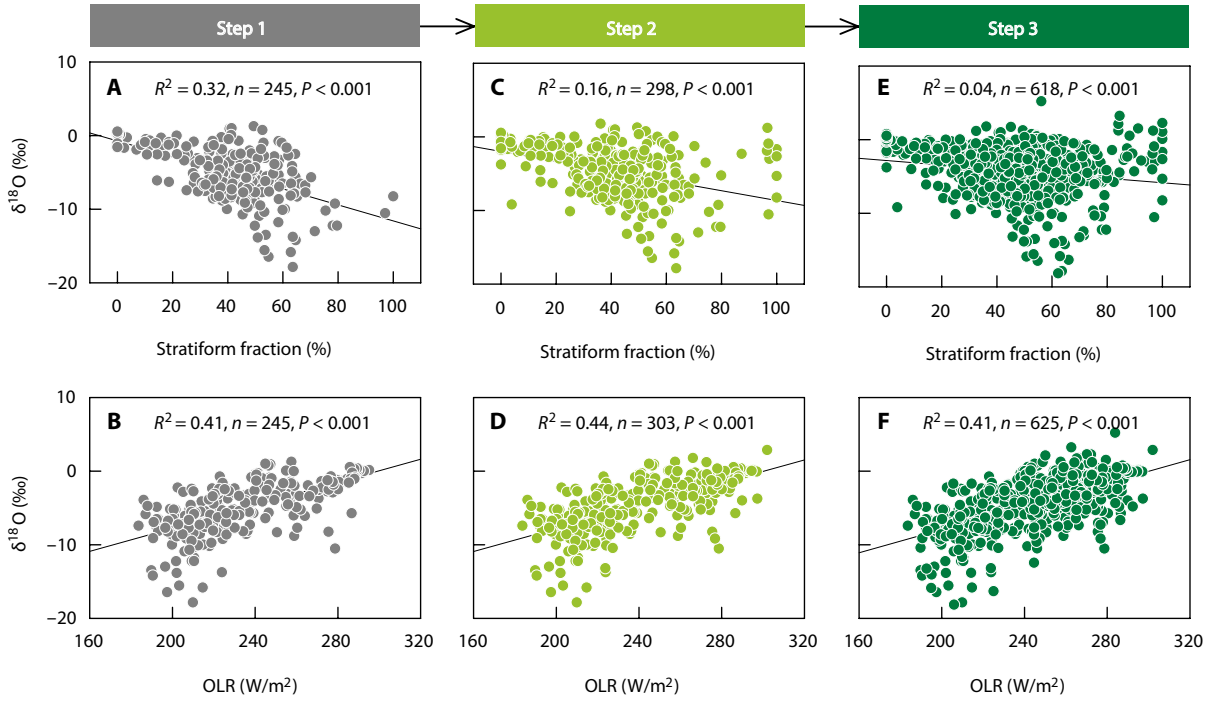

Fig. 3. Correlations of multiyear mean monthly $\delta^{18}O$, stratiform fraction, and OLR in the three steps. (**A** and **B**) Step 1: 26 sites, selected months [i.e. replicated from (*17*)]. (**C** and **D**) Step 2: 26 sites, all months. (**E** and **F**) Step 3: 53 sites, all months (see Materials and Methods).

is less than 50% (*31*)]. Generally, most convective precipitation falls from cumulus or cumulonimbus clouds, while most stratiform precipitation falls from nimbostratus clouds (*32*). The distinction between convective and stratiform precipitation is important to measure to forecast precipitation accurately and to evaluate the effects of tropical convection on global circulation. Satellite observation provides an effective approach for this purpose (*31*, *33*). However, it is very difficult to distinguish convective precipitation from stratiform precipitation using water isotope ratios because high isotopic values can occur in stratiform precipitation. In addition to our findings above, some previous studies in the pantropics (fig. S5) have also shown that isotope ratios in stratiform (convective) precipitation can exhibit high (low) values under different conditions (*18*, *34*–*38*).

During observations of relatively long continuous precipitation events, it is easy to see the apparent differences in isotope ratios of precipitation samples with different rain types. For example, observations from Sumatera (Indonesia) showed that the highest isotope ratio (the average was as high as −3.9‰) appeared in stratiform precipitation rather than convective precipitation (the average was as low as −40.5‰) (*34*). Hence, isotope ratios in precipitation have no connection with rain types (*34*). This argument was also made using similar analyses at Windhoek (*18*) because all abnormally isotope enrichment (as high as 6.4‰, 7.1‰, and 7.3‰) occurred within stratiform precipitation. The observations at Gadanki (southern India) also demonstrated that the convective precipitation $\delta^{18}O$ was relatively low (as low as −13.3‰); however, the stratiform precipitation $\delta^{18}O$ had a wider distribution range with values as high as −1.2‰ (*35*).

Observations from squall line systems also yield similar findings. For instance, stratiform precipitation $\delta^{18}O$ values from one of the four squall lines over the Sahel (Niamey) were higher than those from the convection zone (*36*). Stronger evidence was found from the observations in Singapore, where 17 squalls in 2015 were grouped into three classes (V, W, and other types according to the patterns of the $\delta^{18}O$) (*37*). For the V pattern, the final $\delta^{18}O$ values in the stratiform zone could be higher than the initial values in the convective zone, although most of the lowest $\delta^{18}O$ values occurred within the stratiform zone. For the W pattern, the lowest $\delta^{18}O$ value in a single event could occur in either the convective or stratiform zones. In particular, for the other type patterns, the $\delta^{18}O$ value gradually increases throughout the stratiform zone of the squalls. In the three different classes, the $\delta^{18}O$ almost always has an increasing trend in the last stage of the stratiform zone (*37*).

Likewise, similar results have been reported in observations from hurricane systems. The study on isotopic variability in Hurricane Harvey (2017) precipitation across central Texas indicated that an abrupt and positive shift in $\delta^{18}O$ occurred within the stratiform region (*38*). Broader evidence comes from the daily and monthly observations at some sites as listed in tables S1, S2, and S5. At these sites (fig. S5), some isotope ratios of stratiform precipitation (the stratiform fraction is equal to 100%) contain positive values (>0‰). These high-resolution observations and the broader evidence (fig. S5) further confirm that stratiform precipitation can be associated with high stable isotope values.

Potential causes of isotope enrichment in stratiform precipitation

There are many reasons that can explain the relatively high $\delta^{18}O$ values observed in stratiform precipitation. First, as mentioned above, the $\delta^{18}O$ variations in stratiform precipitation are highly dependent on the intensity of convection (Figs. 2 and 3). Numerous observations (*22*, *36*, *39*, *40*) and simulations (*21*, *41*, *42*) on isotope ratios in stratiform precipitation in the pantropics are almost exclusively carried out in organized convective systems, such as squall lines (*3*, *36*, *42*, *43*), tropical cyclones (*43*–*48*), mesoscale convective systems (*39*, *49*, *50*), and large-scale convective systems (*40*, *51*). Moreover, most of those studies were designed to examine how convection influences the variability of isotope ratios in precipitation.

In many cases, stratiform precipitation is inseparable from deep convection as the convection-generated cumulonimbus clouds not only are the most important cloud in the pantropics but also act as a genitus mother cloud to the precipitating stratiform cloud (nimbostratus) (Fig. 4) (*33*, *52*). The nimbostratus is usually a cloud deck currently or previously extruding out of the cumulonimbus ("nimbostratus cumulonimbogenitus"). Hence, cumulonimbus clouds contain an evolving pattern of newer and older precipitation (*33*). The younger portions of the cumulonimbus are too violent to produce stratiform precipitation. In regions of older deep convection, however, the vertical air motions are generally weaker, and stratiform clouds can form from the cumulonimbus (Fig. 4) (*33*). Hence, the convective and stratiform precipitation both usually occur within the same complex of convection-generated cumulonimbus clouds that are partly convective and partly stratiform (*33*).

A large number of studies (*3*, *11*, *14*–*16*, *36*, *39*, *40*, *52*, *53*) and this study confirm that variations in isotope ratios in precipitation are significantly correlated with the intensity of convection. How convection causes the variability of precipitation isotope ratios has been long debated, and some scientists have put forward different theories (*1*, *3*, *16*, *36*, *39*, *40*, *54*, *55*). Among them, the condensation processes/condensation altitude theory is the most long-standing and widely accepted. Within deep convective systems, condensation can occur up to the tropopause level and imprint highly depleted signatures on the convective precipitation (*3*, *46*, *47*, *52*, *56*). In contrast, the condensate forming the precipitation at lower condensation altitudes is less depleted as the water vapor is less depleted due to previous condensation (*11*, *14*–*16*, *52*, *54*). Simulations across the pantropics also demonstrated that the weakening of deep convection systems can lead to a reduction of net condensation and result in an enrichment of the vapor with heavier isotopes in the lower troposphere (*41*). As a consequence, the subsequent precipitation in the pantropics would contain relatively enriched heavier isotopes (Fig. 4).

As mentioned above, in mesoscale convective (or organized convection or large-scale convective) systems, stratiform clouds derive most of their air mass from convective clouds and so isotope ratios in stratiform precipitation can inherit the signals of convective precipitation. The degree of the enrichment or depletion of convective precipitation isotope ratios is directly controlled by the strength of convection. Therefore, convection plays a decisive role that shapes the initial values of the stratiform precipitation isotope ratios. Here, we call this effect of convection the "imprinting effect" (Fig. 4). Thus, even when the stratiform fraction is as high as 100%, isotope ratios of stratiform precipitation on daily and monthly scales still display a significant correlation with the corresponding convection intensity (fig. S6). Both end members of convective precipitation (the stratiform fraction is 0%) and stratiform precipitation (the stratiform fraction is 100%) have a similarly wide range of isotope ratios as both forms are closely related to convection intensity. Moreover, stratiform precipitation in the pantropics usually occurs simultaneously

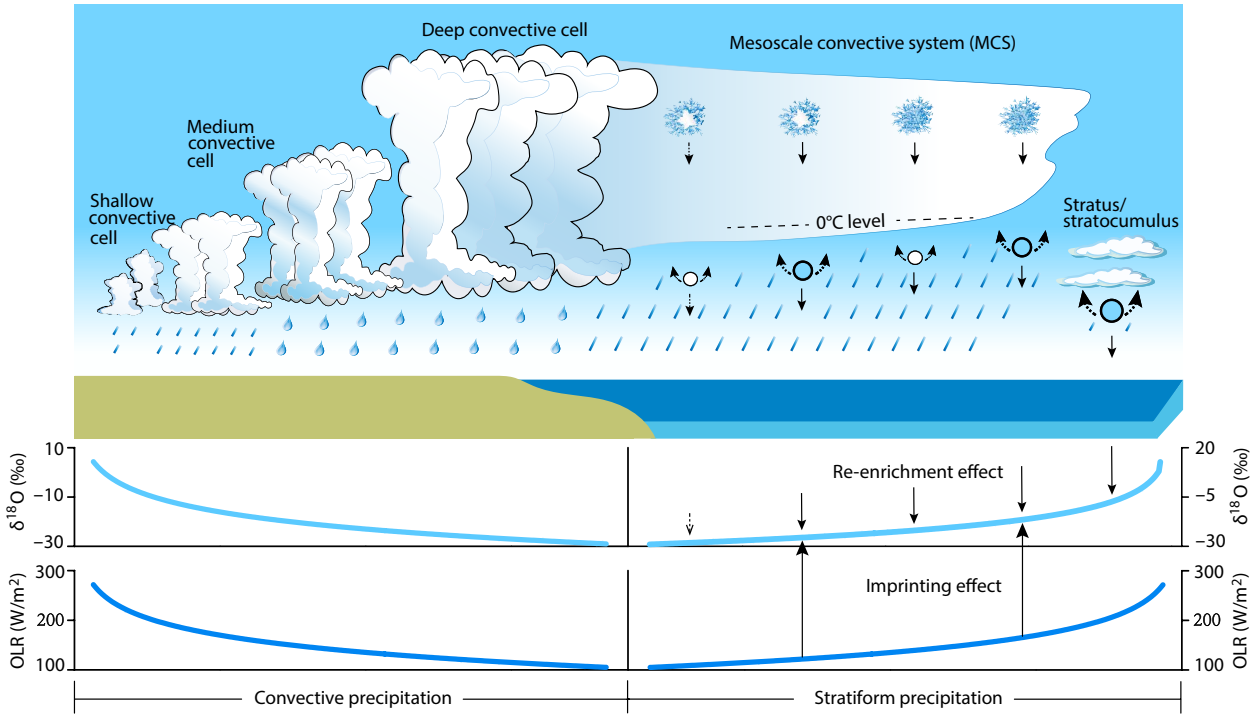

Fig. 4. Schematic representation of the mechanisms that cause isotope enrichment in stratiform precipitation. [Adapted from (*32*, *37*, *52*)] Similar to those in convective precipitation, isotope ratios in stratiform precipitation also span a wide range and are even higher sometimes due to the combined impacts of the imprinting effect (upward straight arrows) and re-enrichment effect (downward straight arrows). Solid (open) ice crystals represent the WBF (no WBF) process. Solid (open) circles with upward curved arrows represent the strong (weak) reevaporation process.

with convective precipitation. These results make it difficult to use isotopic approaches to identify convective and stratiform precipitation.

Second, in addition to the effect of convection on the initial isotope values of stratiform precipitation (imprinting effect), isotope ratios in stratiform precipitation are also closely correlated with the precipitation formation processes in the stratiform region. These processes include the Wegener-Bergeron-Findeisen (WBF) condensation process that occurs above the melt layer (*57*) and the reevaporation process that occurs below the melt layer (*17*). These processes can further enrich isotope ratios in stratiform precipitation (we term the "re-enrichment effect") (Fig. 4).

The effect of the WBF consists of two phase transitions—evaporation of droplets and condensation of vapor into ice—both of which are associated with kinetic fractionation (*58*). In the mixed-phase environment, the effective fractionation over liquid is larger than over ice at cold temperatures when the kinetic effects are strong (*57*, *58*). Under these conditions [in the case of $\delta^{18}O$, the temperature is below −15°C and the updraft velocity is low enough (*57*)], the net result is that the WBF process leads to local isotopic enrichment of water vapor (*57*). It should be noted that the WBF process has limited significance in convective clouds (*59*) but can become important where convective clouds decay to stratiform clouds at the convective detrainment levels (i.e., when strong convection enters its dissipating stage) (*57*). Hence, the subsequent condensation of ice from such vapor would lead to more enriched isotope ratios in the stratiform region. The observation of isotopic changes during Hurricane Harvey (2017) demonstrated that the WBF process drives the more enriched isotope ratios within the stratiform region, which contained decaying convective cells (*38*). Both modeling and observations indicate that the WBF process can result in enriched isotope ratios in stratiform precipitation.

In addition, convective and stratiform precipitation has different reevaporation processes that can lead to different magnitudes of the enrichment in heavier isotopes. Stratiform precipitation consists of small raindrops (~1 mm in diameter), which may partially evaporate or grow by accretion and coalescence (*32*). In comparison, convective precipitation consists of larger raindrops (>2 mm in diameter) that experience little evaporation or growth (*32*, *60*). Clearly, raindrop reevaporation and isotopic exchange with below cloud vapor are more effective in stratiform precipitation compared to convective precipitation due to the smaller raindrop size, increased travel time from the cloud base to ground surface, and decreased average precipitation rate (*18*, *51*). Hence, it is easier for the stratiform precipitation to become enriched in heavier isotopes due to raindrop reevaporation (*51*), even in humid areas (*37*).

The possible occurrence of the WBF process above the melt layer and/or the reevaporation process below the melt layer means that at least four combinations are likely to occur (Fig. 4). Specifically, (i) if the WBF process does not occur during the precipitation formation process, and meanwhile the reevaporation process is very weak, isotope ratios in stratiform precipitation tend to be depleted; (ii) if there is no WBF process, but the raindrops undergo the strong reevaporation process with unsaturated water vapor below the melt layer, isotope ratios in stratiform precipitation may become enriched; (iii) if the WBF process occurs, stratiform precipitation isotope ratios will

likely increase, even if the raindrops do not undergo the strong reevaporation process (*38*); and (iv) if both the WBF and the strong reevaporation processes occur, then enriched isotope ratios in stratiform precipitation are more likely to appear. In addition, when the original convective clouds decay to stratiform clouds (no precipitation falls from convective clouds) and the WBF and/or reevaporation processes are strong, the probability of enriched isotope ratios in stratiform precipitation from such clouds will greatly increase. It is evident that this re-enrichment effect has the opportunity to further enrich isotope ratios within stratiform precipitation. Those findings explain why isotope ratios in stratiform precipitation at some pantropical locations can be higher than those in convective precipitation.

We note that stratiform clouds as mentioned above are mainly nimbostratus clouds that are associated with deep convection. Most stratiform precipitation falls from nimbostratus clouds that reach well above the 0°C level (*32*). There is one exception for stratiform precipitation that includes stratus and stratocumulus cloud decks, which are considered stratiform under standard terminology (*61*), but such clouds occur outside the deep convection system (Fig. 4). These extensive stratiform clouds have tops well below the 0°C level and may produce drizzle or light rain (*60*). These stratiform clouds are very low in height and high in temperature and have raindrop sizes that are very small. Therefore, isotope ratios in such stratiform precipitation become enriched due to the reevaporation process (re-enrichment effect) (Fig. 4).

Last, we emphasize that, although precipitation isotope ratios are sensitive to proportions of convective and stratiform precipitation in some regions (*22*, *23*, *25*, *41*), the rationale behind the phenomenon is still driven by changes in convection intensity (*36*, *39*–*41*, *62*, *63*). From the perspective of simulations, the results of the IsoCAM3.0 model show that isotope ratios in pantropical precipitation are significantly and negatively correlated with the strength of deep convection and indicate that, in turn, the strength of deep convection is responsible for the sensitivity of rain type proportions to precipitation isotope ratios (*41*). From the perspective of the spaceborne measurements over the tropics, the analysis of water vapor isotopes retrieved from TES (Tropospheric Emission Spectrometer) onboard the NASA Aura and IASI (Infrared Atmospheric Sounding Interferometer) onboard the MetOp satellite and latent heating product derived from the TRMM precipitation radar (PR) also demonstrate that the depth of convection is controlling the relationship between the stratiform fraction and water vapor isotope ratios in the tropics (*63*). We also found that, when the stratiform fraction is greater than 60%, the water vapor isotope ratios from the spaceborne measurements change very little and even slightly increase with increasing stratiform fraction. This result supports our findings based on observations of precipitation isotope ratios in the pantropics—that is, when the stratiform fraction is greater than 60% on different timescales, precipitation isotope ratios in the pantropics slightly increase.

On the basis of the extensive databases, we found that precipitation isotope ratios in the pantropics are independent of the stratiform fraction whether on daily, monthly, or even annual timescales because isotope ratios in stratiform precipitation span a wide range. Hence, variations in isotope ratios in pantropical precipitation cannot be attributed to rain types. By contrast, changes in isotope ratios in pantropical precipitation were correlated with the intensity of convection across the different timescales, which imprint specific signatures on both convective and stratiform precipitation (imprinting effect). While reduced convection can cause isotope enrichment in stratiform precipitation, the WBF and raindrop reevaporation processes can also drive stratiform precipitation isotope ratios to become further enriched (re-enrichment effect).

Our work discusses the serious weaknesses of the SF theory that researchers should consider if applying it to stable isotope datasets in the future. While our study focused on convection combined with the WBF and raindrop reevaporation processes, we acknowledge that isotope ratios in pantropical precipitation are influenced by many other factors including mesoscale downdrafts (*3*, *36*, *39*–*41*), rain-vapor diffusive exchanges (*1*, *42*, *47*, *56*, *64*), and mixing between contrasting air masses (*65*–*68*). From a pantropical perspective, it is clear that the significant correlation between isotope ratios in pantropical precipitation and OLR confirms the important role of the intensity of convection on water isotope ratios. We conclude that water isotope ratios in the pantropics are indicative of the intensity of convection rather than rain type proportions. In addition, the water isotope ratios may also allow us to better understand the complex interplay of moistening and drying that governs the large-scale convective systems such as Madden-Julian Oscillation (*69*). In terms of paleoclimate studies, we emphasize that stable isotope records preserved in paleoclimate archives from the pantropics cannot be used to reconstruct changes in the proportions of convective and stratiform precipitation but rather can be used to reconstruct the history of the intensity of paleoconvection. Apparent contradictions or conflicts that occur in paleoclimate reconstructions cannot be reconciled by rain types.

MATERIALS AND METHODS

The precipitation isotope ratio measurement data were obtained from the published literature, the GNIP database, and Daily Basis Precipitation Sampling Network for Water Isotope Analysis at Indonesia (here we abbreviated it as IDNIP) database. The enrichment of heavy isotopes ($H_2{}^{18}O$ or HDO) is expressed as $\delta^{18}O$ (or $\delta^{2}H$) = ($R_{sample}/R_{SMOW} - 1$) × 1000 in ‰, where R denotes the ratio of $^{18}O/^{16}O$ (or $^{2}H/H$) in a sample relative to the Standard Mean Ocean Water (SMOW) reference. The stratiform fraction data in the pantropics were derived from the new versions of the TRMM PR and GPM DPR satellite data products. The stratiform fraction is the ratio of stratiform to the total surface rain rate. Values range from 0 to 100%. The values of the mean estimated surface precipitation rate range from 0 to 3000 mm/hour (https://gpmweb2https.pps.eosdis.nasa.gov/pub/stout/helpdesk/filespec.GPM.V7.pdf). Generally, the convective intensity is defined by updraft magnitude (*70*). Here, we used OLR to indicate the convective intensity because it is difficult for satellites to measure the updraft speed (*70*). The lower the OLR, the stronger the convection. The daily, monthly, annual, and multiyear mean monthly OLR data were calculated by the mean top net longwave radiation flux data, which were obtained from the ERA5 reanalysis with a spatial resolution of 0.25° × 0.25° and a temporal resolution of 1 hour. The calculated OLR data were validated by the daily OLR data with a spatial resolution of 1° × 1° provided by the National Oceanic and Atmospheric Administration (NOAA) National Centers for Environmental Information (NCEI) (fig. S7).

The choice of sites and data on the daily timescale

We compiled the published daily $\delta^{18}O$ and the corresponding precipitation amount data (covering the period of 1998 to 2021) for 105 sites across the pantropics (35°N to 35°S). We then selected the

valid sites based on the availability of the corresponding stratiform fraction data (as follows).

On the daily timescale, the stratiform fraction data were obtained from GPM 3GCSH TRMM V07 (which replaces the old TRMM legacy product TRMM 3G31, which is a 0.25° gridded dataset with 1.5-hour intervals, covering 37°N to 37°S horizontally) from 1 January 1998 to 18 March 2014 and GPM 3GCSH V07 from 19 March 2014 to 31 December 2021 (which is a 0.5° gridded data with 1.5-hour intervals, covering 65°N to 65°S horizontally). It should be noted that the data products of TRMM PR and GPM DPR have similar temporal resolution of 16 orbits a day with swath widths of 245 km (but 215 km for TRMM PR during 27 November 1997 to 6 August 2001, prior to orbit boost) (*18*, *24*, *71*). This means that at least 164 orbits are needed to cover the whole equator (roughly 40,000 km) corresponding to around 10 days based on the swath width (*24*). As a consequence, for a given precipitation sampling site, the daily data products of TRMM and GPM do not have the corresponding stratiform fraction data for each precipitation day. On the daily timescale, our data selection criteria is that the published daily $\delta^{18}O$ data cover the period of 1998 to 2021 across the regions of 35°N to 35°S, and the valid sample size (n) at each site is required to not be less than 12 (i.e., $n \geq 12$) during the correlation analysis of the stratiform fraction–$\delta^{18}O$ relationship. In that case, only 38 of the 105 sites met the criteria (Fig. 1, black crosses, and table S1).

The choice of sites and data on the monthly timescale

According to the criteria of the study of the SF theory (*17*), we selected the pantropical sites located in the 35°N to 35°S latitude range with a minimum of four consecutive years of isotope data in the 1998 to 2014 period (*17*). In this way, the monthly $\delta^{18}O$ and the corresponding precipitation amount data at 51 sites were retrieved from the GNIP database, and data from two other sites (Jambi and Kototabang) were obtained from the IDNIP database.

On the basis of the criteria, we eliminated four sites (Jakarta, Manila, Vienna, and Krakow) previously included in the study of the SF theory (*17*) because the observed $\delta^{18}O$ data from Jakarta (covering the period of January 1962 to December 1997) and Manila (covering the period of January 1961 to December 1976) do not overlap with the stratiform fraction data (covering the period of January 1998 to October 2014), and another two mid-latitude sites of Vienna (48.25°N, 16.36°E, 198 m above sea level) and Krakow (50.06°N, 19.85°E, 205 m above sea level) were beyond the specified latitudinal range of this study. Overall, we selected 26 valid sites from the study of the SF theory (Fig. 1, green dots) (*17*). In addition, we added another 27 GNIP sites that also meet the criteria proposed by the study of the SF theory (*17*) but were missed in that study (Fig. 1, yellow dots). In total, we retrieved monthly $\delta^{18}O$ and the corresponding precipitation amount data from 53 sites (table S2). Unlike the choice of the $\delta^{18}O$ data in the study of the SF theory (*17*), we used complete data, which cover all months.

In comparison with the study of the SF theory (*17*), which used the stratiform fraction data from TRMM 2A25 with a relatively coarser spatial resolution of 2.5° grid cell, in this study, we obtained the stratiform fraction data for the 53 sites from TRMM 3H31 with a higher spatial resolution of 0.5° gridded data, covering 37°N to 37°S horizontally. Some precipitation sampling sites were located in close proximity, and some sites were even within the same grid cell. Hence, the stratiform fraction data for two adjacent sampling sites could be retrieved from the same grid cell, which can result in a large bias in calculations particularly for the data that have a coarser spatial resolution (2.5°). This bias can be reduced to a large extent by using the TRMM 3H31 data with a higher spatial resolution (0.5°).

The choice of sites and data on other timescales

The choices of sites and the $\delta^{18}O$ and the corresponding precipitation amount data combined with the stratiform fraction and OLR data for the 53 sites (table S2) on the annual and multiyear mean monthly timescales were consistent with those on the monthly timescales. Note that the monthly $\delta^{18}O$ values were used to calculate arithmetic means (unweighted) on the annual and multiyear mean monthly timescales.

In addition, to determine if the stratiform fraction data with different temporal resolutions would affect our results, we further calculated the monthly, annual, and annual average monthly stratiform fraction data for the 53 sites from the GPM 3GCSH TRMM V07 and GPM 3GCSH V07 datasets as mentioned above and analyzed the correlations between $\delta^{18}O$ and the stratiform fraction on the monthly, annual, and annual average monthly timescales (see fig. S8 in the Supplementary Materials for details).

Supplementary Materials

This PDF file includes:

Text S1
Figs. S1 to S8
Legends for tables S1 to S5
References

Other Supplementary Material for this manuscript includes the following:

Tables S1 to S5

REFERENCES AND NOTES

1. W. Dansgaard, Stable isotopes in precipitation. *Tellus* **16**, 436–468 (1964).
2. T. Yamanaka, J. Shimada, Y. Hamada, T. Tanaka, Y. Yang, W. Zhang, C. Hu, Hydrogen and oxygen isotopes in precipitation in the northern part of the North China Plain: Climatology and inter-storm variability. *Hydrol. Process.* **18**, 2211–2222 (2004).
3. C. Risi, S. Bony, F. Vimeux, L. Descroix, B. Ibrahim, E. Lebreton, I. Mamadou, B. Sultan, What controls the isotopic composition of the African monsoon precipitation? Insights from event-based precipitation collected during the 2006 AMMA field campaign. *Geophys. Res. Lett.* **35**, L24808 (2008).
4. N. Kurita, K. Ichiyanagi, J. Matsumoto, M. D. Yamanaka, T. Ohata, The relationship between the isotopic content of precipitation and the precipitation amount in tropical regions. *J. Geochem. Explor.* **102**, 113–122 (2009).
5. F. Vimeux, G. Tremoy, C. Risi, R. Gallaire, A strong control of the South American SeeSaw on the intra-seasonal variability of the isotopic composition of precipitation in the Bolivian Andes. *Earth Planet. Sci. Lett.* **307**, 47–58 (2011).
6. S. F. M. Breitenbach, J. F. Adkins, H. Meyer, N. Marwan, K. K. Kumar, G. H. Haug, Strong influence of water vapor source dynamics on stable isotopes in precipitation observed in Southern Meghalaya, NE India. *Earth Planet. Sci. Lett.* **292**, 212–220 (2010).
7. J. W. Moerman, K. M. Cobb, J. F. Adkins, H. Sodemann, B. Clark, A. A. Tuen, Diurnal to interannual rainfall $\delta^{18}O$ variations in northern Borneo driven by regional hydrology. *Earth Planet. Sci. Lett.* **369–370**, 108–119 (2013).
8. H. Oza, V. Padhya, A. Ganguly, K. Saikranthi, T. N. Rao, R. D. Deshpande, Hydrometeorological processes in semi-arid western India: Insights from long term isotope record of daily precipitation. *Clim. Dyn.* **54**, 2745–2757 (2020).
9. M. G. Yadava, R. Ramesh, K. Pandarinath, A positive 'amount effect' in the Sahayadri (Western Ghats) rainfall. *Curr. Sci.* **93**, 560–564 (2007).
10. P. R. Lekshmy, M. Midhun, R. Ramesh, Spatial variation of amount effect over peninsular India and Sri Lanka: Role of seasonality. *Geophys. Res. Lett.* **42**, 5500–5507 (2015).
11. M. A. Scholl, J. B. Shanley, J. P. Zegarra, T. B. Coplen, The stable isotope amount effect: New insights from NEXRAD echo tops, Luquillo Mountains, Puerto Rico. *Water Resour. Res.* **45**, W12407 (2009).

12. R. D. Deshpande, A. S. Maurya, B. Kumar, A. Sarkar, S. K. Gupta, Rain-vapor interaction and vapor source identification using stable isotopes from semiarid western India. *J. Geophys. Res.* **115**, D23311 (2010).
13. Y. Wang, C. Hu, J. Ruan, K. R. Johnson, East Asian precipitation $\delta^{18}O$ relationship with various monsoon indices. *J. Geophys. Res. Atmos.* **125**, e2019JD032282 (2020).
14. D. S. Permana, L. G. Thompson, G. Setyadi, Tropical West Pacific moisture dynamics and climate controls on rainfall isotopic ratios in southern Papua, Indonesia. *J. Geophys. Res. Atmos.* **121**, 2222–2245 (2016).
15. L. G. Thompson, M. E. Davis, E. Mosley Thompson, E. Beaudon, S. E. Porter, S. Kutuzov, P.-N. Lin, V. N. Mikhalenko, K. R. Mountain, Impacts of recent warming and the 2015/2016 El Niño on tropical Peruvian ice fields. *J. Geophys. Res. Atmos.* **122**, 12688–12701 (2017).
16. W. Yu, T. Yao, L. G. Thompson, J. Jouzel, H. Zhao, B. Xu, Temperature signals of ice core and speleothem isotopic records from Asian monsoon region as indicated by precipitation $\delta^{18}O$. *Earth Planet. Sci. Lett.* **554**, 116665 (2021).
17. P. K. Aggarwal, U. Romatschke, L. Araguas-Araguas, D. Belachew, F. J. Longstaffe, P. Berg, C. Schumacher, A. Funk, Proportions of convective and stratiform precipitation revealed in water isotope ratios. *Nat. Geosci.* **9**, 624–629 (2016).
18. K. F. Kaseke, L. Wang, H. Wanke, C. Tian, M. Lanning, W. Jiao, Precipitation origins and key drivers of precipitation isotope (^{18}O, ^{2}H, and ^{17}O) compositions over Windhoek. *J. Geophys. Res. Atmos.* **123**, 7311–7330 (2018).
19. Z. Wei, X. Lee, Z. Liu, U. Seeboonruang, M. Koike, K. Yoshimura, Influences of large-scale convection and moisture source on monthly precipitation isotope ratios observed in Thailand, Southeast Asia. *Earth Planet. Sci. Lett.* **488**, 181–192 (2018).
20. E. Casellasa, J. Latronb, C. Cayuelab, J. Becha, M. Udinaa, Y. Solaa, K.-O. Lee, P. Llorens, Moisture origin and characteristics of the isotopic signature of rainfall in a Mediterranean mountain catchment (Vallcebre, eastern Pyrenees). *J. Hydrol.* **575**, 767–779 (2019).
21. J. Hu, J. Emile-Geay, J. Nusbaumer, D. Noone, Impact of convective activity on precipitation $\delta^{18}O$ in isotope-enabled general circulation models. *J. Geophys. Res. Atmos.* **123**, 13595–13610 (2018).
22. C. Zwart, N. C. Munksgaard, A. Protat, N. Kurita, D. Lambrinidis, M. I. Bird, The isotopic signature of monsoon conditions, cloud modes, and rainfall type. *Hydrol. Process.* **32**, 2293–2451 (2018).
23. B. L. Konecky, D. C. Noone, K. M. Cobb, The influence of competing hydroclimate processes on stable isotope ratios in tropical rainfall. *Geophys. Res. Lett.* **46**, 1622–1633 (2019).
24. N. C. Munksgaard, N. Kurita, R. Sánchez-Murillo, N. Ahmed, L. Araguas, D. L. Balachew, M. I. Bird, S. Chakraborty, N. K. Chinh, K. M. Cobb, S. A. Ellis, G. Esquivel-Hernández, S. Y. Ganyaglo, J. Gao, D. Gastmans, K. F. Kaseke, S. Kebede, M. R. Morales, M. Mueller, S. C. Poh, V. dos Santos, H. Shaoneng, L. Wang, H. Yacobaccio, C. Zwart, Data descriptor: Daily observations of stable isotope ratios of rainfall in the tropics. *Sci. Rep.* **9**, 14419 (2019).
25. R. Sánchez-Murillo, A. M. Durán-Quesada, G. Esquivel-Hernández, D. Roias-Cantillano, C. Birkel, K. Welsh, M. Sánchez-Llull, C. M. Alonso-Hernández, D. Tetzlaff, C. Soulsby, J. Boll, N. Kurita, K. M. Cobb, Deciphering key processes controlling rainfall isotopic variability during extreme tropical cyclones. *Nat. Commun.* **10**, 4321 (2019).
26. S. Sengupta, S. K. Bhattacharya, A. Parekh, S. S. Nimya, K. Yoshimurat, A. Sarkar, Signatures of monsoon intra-seasonal oscillation and stratiform process in rain isotope variability in northern Bay of Bengal and their simulation by isotope enabled general circulation model. *Clim. Dyn.* **55**, 1649–1663 (2020).
27. H. K. Changa, R. D. Gonçalves, P. K. Aggarwal, M. R. Stradiotob, E. C. B. Hespanhol, N. C. Sturchio, U. Romatschke, L. J. A. Araguas, Groundwater isotope ratios reflect convective and stratiform (paleo) precipitation fractions in Brazil. *J. Hydrol.* **585**, 1248 (2020).
28. T. Bhattacharya, R. Feng, J. E. Tierney, C. Rubbelke, N. Burls, S. Knapp, M. Fu, Expansion and intensification of the North American Monsoon during the Pliocene. *AGU Adv.* **3**, e2022AV000757 (2022).
29. B. Chase, C. Harris, M. J. de Wit, J. Kramers, S. Doel, J. Stankiewicz, South African speleothems reveal influence of high- and low-latitude forcing over the past 113.5 k.y. *Geology* **49**, 1353–1357 (2021).
30. R. M. Sullivan, P. J. van Hengstum, J. P. Donnelly, A. E. Tamalavage, T. S. Winkler, S. N. Little, L. Mejia-Ortiz, E. G. Reinhardt, S. Meacham, C. Schumacher, R. Korty, Northeast Yucatan hurricane activity during the Maya Classic and Postclassic periods. *Sci. Rep.* **12**, 20107 (2022).
31. C. Schumacher, A. Funk, Assessing convective-stratiform precipitation regimes in the tropics and extratropics with the GPM satellite radar. *Geophys. Res. Lett.* **50**, e2023GL102786 (2023).
32. R. A. Houze Jr., "Nimbostratus and the separation of convective and stratiform precipitation" in *Cloud Dynamics*, vol. 104, *International Geophysics*, R. A. Houze, Ed. (Academic Press, 2014), pp. 141–163.
33. R. A. Houze Jr., Stratiform precipitation in regions of convection: A meteorological paradox? *Bull. Am. Meteorol. Soc.* **78**, 2179–2196 (1997).
34. H. Fudeyasu, K. Ichiyanagi, K. Yoshimura, S. Mori, J. Hamada, N. Sakurai, M. D. Yamanaka, J. Matsumoto, F. Syamsudin, Effects of large-scale moisture transport and mesoscale processes on precipitation isotope ratios observed at Sumatera, Indonesia. *J. Meteor. Soc. Japan* **89A**, 49–59 (2011).
35. S. R. Managave, R. A. Jani, T. N. Rao, K. Sunilkumar, S. Satheeshkumar, R. Ramesh, Intra-event isotope and raindrop size data of tropical rain reveal effects concealed by event averaged data. *Clim. Dyn.* **47**, 981–987 (2016).
36. C. Risi, S. Bony, F. Vimeux, M. Chong, L. Descroix, Evolution of the stable water isotopic composition of the rain sampled along Sahelian squall lines. *Q. J. R. Meteorol. Soc.* **136**, 227–242 (2010).
37. S. He, N. F. Goodkin, N. Kurita, X. Wang, C. M. Rubin, Stable isotopes of precipitation during tropical Sumatra Squalls in Singapore. *J. Geophys. Res. Atmos.* **123**, 3812–3829 (2018).
38. C. Sun, L. Tian, T. M. Shanahan, J. W. Partin, Y. Gao, N. Piatrunia, J. Banner, Isotopic variability in tropical cyclone precipitation is controlled by Rayleigh distillation and cloud microphysics. *Commun. Earth Environ.* **3**, 50 (2022).
39. N. Kurita, Water isotopic variability in response to mesoscale convective system over the tropical ocean. *J. Geophys. Res. Atmos.* **118**, 10376–10390 (2013).
40. N. Kurita, D. Noone, C. Risi, G. A. Schmidt, H. Yamada, K. Yoneyama, Intraseasonal isotopic variation associated with the Madden-Julian Oscillation. *J. Geophys. Res.* **116**, D24101 (2011).
41. T. Tharammal, G. Bala, D. Noone, Impact of deep convection on the isotopic amount effect in tropical precipitation. *J. Geophys. Res. Atmos.* **122**, 1505–1523 (2017).
42. C. Risi, C. Muller, F. Vimeux, P. Blossey, G. Védeau, C. Dufaux, S. Abramian, What controls the mesoscale variations in water isotopic composition within tropical cyclones and squall lines? Cloud resolving model simulations in radiative-convective equilibrium. *J. Adv. Model. Earth Syst.* **15**, e2022MS003331 (2023).
43. G. Tremoy, F. Vimeux, S. Soumana, I. Souley, C. Risi, G. Favreau, M. Oï, Clustering mesoscale convective systems with laser-based water vapor $\delta^{18}O$ monitoring in Niamey (Niger). *J. Geophys. Res. Atmos.* **119**, 5079–5103 (2014).
44. S. Chakraborty, N. Sinha, R. Chattopadhyay, S. Sengupta, P. M. Mohan, A. Datyel, Atmospheric controls on the precipitation isotopes over the Andaman Islands, Bay of Bengal. *Sci. Rep.* **6**, 19555 (2016).
45. D. Jackisch, B. Yeo, A. D. Switzer, S. He, D. L. M. Cantarero, F. P. Siringan, N. F. Goodkin, Precipitation stable isotopic signatures of tropical cyclones in Metropolitan Manila, Philippines, show significant negative isotopic excursions. *Nat. Hazards Earth Syst. Sci.* **22**, 213–226 (2022).
46. J. R. Lawrence, S. D. Gedzelma, Low stable isotope ratios of tropical cyclone rains. *Geophys. Res. Lett.* **23**, 527–530 (1996).
47. J. R. Lawrence, S. D. Gedzelman, D. Dexheimer, H.-K. Cho, G. D. Carrie, R. Gasparini, C. R. Anderson, K. P. Bowman, M. I. Biggerstaff, Stable isotopic composition of water vapor in the tropics. *J. Geophys. Res.* **109**, D06115 (2004).
48. R. M. Price, P. K. Swart, H. E. Willoughby, Seasonal and spatial variation in the stable isotopic composition ($\delta^{18}O$ and δD) of precipitation in south Florida. *J. Hydrol.* **358**, 193–205 (2008).
49. T. N. Rao, B. Radhakrishna, R. Srivastava, T. M. Satyanarayana, D. N. Rao, R. Ramesh, Inferring microphysical processes occurring in mesoscale convective systems from radar measurements and isotopic analysis. *Geophys. Res. Lett.* **35**, L09813 (2008).
50. C. R. Maupin, E. B. Roark, K. Thirumalai, C. Shen, C. Schumacher, S. V. Kampen-Lewis, A. L. Housson, C. L. McChesney, O. Baykara, T.-L. Yu, K. White, J. W. Partin, Abrupt Southern Great Plains thunderstorm shifts linked to glacial climate variability. *Nat. Geosci.* **14**, 396–401 (2021).
51. P. R. Lekshmy, M. Midhun, R. Ramesh, Influence of stratiform clouds on δD and $\delta^{18}O$ of monsoon water vapour and rain at two tropical coastal stations. *J. Hydrol.* **563**, 354–362 (2018).
52. R. A. Houze Jr., 100 years of research on mesoscale convective systems. *Meteorol. Monogr.* **59**, 17.1–17.54 (2018).
53. H. Celle-Jeantona, R. Gonfiantini, Y. Travia, B. Sol, Oxygen-18 variations of rainwater during precipitation: Application of the Rayleigh model to selected rainfalls in Southern France. *J. Hydrol.* **289**, 165–177 (2004).
54. Z. Cai, L. Tian, Atmospheric controls on seasonal and interannual variations in the precipitation isotope in the East Asian Monsoon region. *J. Clim.* **29**, 1339–1352 (2016).
55. M. Moore, Z. Kuang, P. N. Blossey, A moisture budget perspective of the amount effect. *Geophys. Res. Lett.* **41**, 1329–1335 (2014).
56. J.-E. Lee, I. Fung, "Amount effect" of water isotopes and quantitative analysis of post-condensation processes. *Hydrol. Process.* **22**, 1–8 (2008).
57. M. Bolot, B. Legras, E. J. Moyer, Modelling and interpreting the isotopic composition of water vapour in convective updrafts. *Atmos. Chem. Phys.* **13**, 7903–7935 (2013).
58. P. Ciais, J. Jouzel, Deuterium and oxygen 18 in precipitation: Isotopic model, including mixed cloud processes. *J. Geophys. Res.* **99**, 16793–16803 (1994).
59. A. Korolev, Limitations of the Wegener-Bergeron-Findeisen mechanism in the evolution of mixed-phase clouds. *J. Atmos. Sci.* **64**, 3372–3375 (2006).

60. C. Schumacher, R. A. Houze Jr., Stratiform rain in the tropics as seen by the TRMM precipitation radar. *J. Clim.* **16**, 1739–1756 (2003).
61. T. S. Glickman, *Glossary of Meteorology* (American Meteorological Society, ed. 2, 2000).
62. G. Torri, D. Ma, Z. Kuang, Stable water isotopes and large-scale vertical motions in the tropics. *J. Geophys. Res. Atmos.* **122**, 3703–3717 (2017).
63. J.-L. Lacourd, C. Risi, J. Worden, C. Clerbaux, P.-F. Coheurd, Importance of depth and intensity of convection on the isotopic composition of water vapor as seen from IASI and TES δD observations. *Earth Planet. Sci. Lett.* **481**, 387–394 (2018).
64. R. D. Field, D. B. A. Jones, D. P. Brown, Effects of postcondensation exchange on the isotopic composition of water in the atmosphere. *J. Geophys. Res.* **115**, D24305 (2010).
65. J. Worden, D. Noone, K. Bowman, Importance of rain evaporation and continental convection in the tropical water cycle. *Nature* **445**, 528–532 (2007).
66. D. Brown, J. Worden, D. Noone, Comparison of atmospheric hydrology over convective continental regions using water vapor isotope measurements from space. *J. Geophys. Res.* **113**, D15124 (2008).
67. J. Galewsky, J. V. Hurley, An advection-condensation model for subtropical water vapor isotopic ratios. *J. Geophys. Res.* **115**, D16116 (2010).
68. M. Benetti, G. Aloisi, G. Reverdin, C. Risi, G. Sèze, Importance of boundary layer mixing for the isotopic composition of surface vapor over the subtropical North Atlantic Ocean. *J. Geophys. Res. Atmos.* **120**, 2190–2209 (2015).
69. S. Dee, A. Bailey, J. L. Conroy, A. Atwood, S. Stevenson, J. Nusbaumer, D. Noone, Water isotopes, climate variability, and the hydrological cycle: Recent advances and new frontiers. *Environ. Res. Clim.* **2**, 022002 (2023).
70. H. Jiang, The relationship between tropical cyclone intensity change and the strength of inner-core convection. *Mon. Weather Rev.* **140**, 1164–1176 (2012).
71. H.-K. Lee, M.-J. Kang, H.-Y. Chun, D. Kim, D.-B. Shin, Characteristics of latent heating rate from GPM and convective gravity wave momentum flux calculated using the GPM data. *J. Geophys. Res. Atmos.* **127**, e2022JD037003 (2022).
72. M. R. Islam, J. Gao, N. Ahmed, M. M. Karim, A. Q. Bhuiyan, A. Ahsan, S. Ahmed, Controls on spatiotemporal variations of stable isotopes in precipitation across Bangladesh. *Atmos. Res.* **247**, 105224 (2021).
73. H. Wu, X. Zhang, X. Li, G. Li, Y. Huang, Seasonal variations of deuterium and oxygen-18 isotopes and their response to moisture source for precipitation events in the subtropical monsoon region. *Hydrol. Process.* **29**, 90–102 (2015).
74. S. Chakraborty, P. K. D. Burman, D. Sarma, N. S. A. Datye, A. Metya, C. Murkute, S. K. Saha, K. Sujith, N. Gogoi, A. Bora, S. Maji, D. K. Parua, S. Bera, Linkage between precipitation isotopes and biosphere-atmosphere interaction observed in northeast India. *NPJ Clim. Atmos. Sci.* **5**, 1–10 (2022).
75. S. Acharya, X. Yang, T. Yao, D. Shrestha, Stable isotopes of precipitation in Nepal Himalaya highlight the topographic influence on moisture transport. *Quat. Int.* **565**, 22–30 (2020).
76. X. Yang, M. E. Davis, S. Acharya, T. Yao, Asian monsoon variations revealed from stable isotopes in precipitation. *Clim. Dyn.* **51**, 2267–2283 (2018).
77. X. Wu, X. Zhu, M. Pan, M. Zhang, Seasonal variability of oxygen and hydrogen stable isotopes in precipitation and cave drip water at Guilin, southwest China. *Environ. Earth Sci.* **72**, 3183–3191 (2014).
78. J. Gou, S. Qu, H. Guan, P. Shi, Z. Su, Z. Lin, J. Liu, J. Zhu, Relationship between precipitation isotopic compositions and synoptic atmospheric circulation patterns in the lower reach of the Yangtze River. *J. Hydrol.* **605**, 127289 (2022).
79. C. U. Warrier, M. P. Babu, M. Sudheesh, R. D. Deshpande, Studies on stable isotopic composition of daily rainfall from Kozhikode, Kerala, India. *Isotopes Environ. Health Stud.* **52**, 1–12 (2015).
80. J. Crawford, S. E. Hollins, K. T. Meredith, C. E. Hughes, Precipitation stable isotope variability and subcloud evaporation processes in a semi-arid region. *Hydrol. Process.* **31**, 20–34 (2017).
81. A. A. Fousiya, G. H. Aravind, H. Achyutan, S. Chakraborty, R. Chattopadhyay, A. Datye, C. Murkute, A. M. Lone, R. H. Kripalani, M. G. Yadava, P. M. Mohan, Modulation of the precipitation isotopes by the dynamic and thermodynamic variables of the atmosphere in southern parts of India. *Water Resour. Res.* **58**, e2021WR030855 (2022).
82. Z. Zhan, H. Pang, S. Wu, Z. Liu, W. Zhang, T. Xu, H. Cheng, S. Hou, Determining key upstream convection and rainout zones affecting $\delta^{18}O$ in water vapor and precipitation based on 10-year continuous observations in the East Asian Monsoon region. *Earth Planet. Sci. Lett.* **601**, 117912 (2023).
83. V. Santos, D. Gastmans, R. Sanchez-Murillo, L. F. Gozzo, L. V. Batista, R. L. Manzione, J. Martinez, Regional atmospheric dynamics govern interannual and seasonal stable isotope composition in southeastern Brazil. *J. Hydrol.* **579**, 124136 (2019).
84. J. Cai, Y. Yang, Z. Yang, W. Qiu, X. Jiang, Isotope composition of daily precipitation from 2019 to 2020 in Sanming, southeastern China. *Front. Environ. Sci.* **10**, 1061882 (2022).
85. C. J. Eastoe, D. L. Dettman, Isotope amount effects in hydrologic and climate reconstructions of monsoon climates: Implications of some long-term data sets for precipitation. *Chem. Geol.* **430**, 78–89 (2016).
86. S. Tao, X. Zhang, G. Pan, J. Xu, Z. Zeng, Moisture source identification based on the seasonal isotope variation of precipitation in the Poyang Lake Wetland, China. *J. Hydrol.* **37**, 100892 (2021).
87. F. Chen, C. Huang, Q. Lao, S. Zhang, C. Chen, X. Zhou, X. Lu, Q. Zhu, Typhoon control of precipitation dual isotopes in southern China and its palaeoenvironmental implications. *J. Geophys. Res. Atmos.* **126**, e2020JD034336 (2021).

Acknowledgments: We thank M. Bolot for helpful discussions. **Funding:** This work was funded by the Basic Science Center for Tibetan Plateau Earth System (NSFC project no. 41988101-03), the Second Tibetan Plateau Scientific Expedition and Research Program (2019QZKK0201), and the National Natural Science Foundation of China (NSFC) (42171122). **Author contributions:** Conceptualization: W.Y. Formal analysis: W.Y., R.G., J.Z., J.H., X.Z., and W.T. Data curation: W.Y., R.G., J.Z., J.H., X.Z., and W.T. Visualization: W.Y. and R.G. Supervision: W.Y. Writing—original draft: W.Y., L.G.T., S.L., J.Z., Z.J., Y.M., B.X., G.W., Q.W., X.Z., P.R., Z.Z., and D.Q. Writing—review and editing: W.Y., L.G.T., and S.L. **Competing interests:** The authors declare that they have no competing interests. **Data and materials availability:** All data needed to evaluate the conclusions in the paper are present in the paper and/or the Supplementary Materials. Daily stable isotopes and precipitation amount data were obtained from the published literature (see table S1). Monthly stable isotopes and precipitation amount data at the 24 GNIP sites were retrieved from the GNIP database (https://iaea.org/services/networks/gnip). Monthly stable isotopes and precipitation amount data at two other sites of Jambi and Kototabang were obtained from "Daily Basis Precipitation Sampling Network for Water Isotope Analysis at Indoneshia" at the Institute of Observational Research for Global Change, Japan Agency for Marine-Earth Science and Technology, by N. Kurita and K. Ichiyanagi (https://ads.nipr.ac.jp/data/meta/C20100906-005). Daily stratiform fractions for the period of 1998 to 2021 were obtained from NASA's GPM 3GCSH TRMM v07 (1 January 1998 to 18 March 2014) (https://disc.gsfc.nasa.gov/datasets/GPM_3GCSH_TRMM_07/summary?keywords=3GCSHT) and NASA's GPM 3GCSH v07 (19 March 2014 to 31 December 2021) (https://disc.gsfc.nasa.gov/datasets/GPM_3GCSH_07/summary?keywords=3GCSHT). Monthly stratiform fractions for the period of 1998 to 2014 were obtained from NASA's TRMM 3H31 v7 (https://disc.gsfc.nasa.gov/datasets/TRMM_3H31_7/summary?keywords=3H31). The Copernicus Climate Change Service provided the mean top net longwave radiation flux data (https://cds.climate.copernicus.eu/cdsapp#!/dataset/reanalysis-era5-single-levels?tab=form). The NOAA NCEI provided the daily OLR data (https://ncei.noaa.gov/products/climate-data-records/outgoing-longwave-radiation-daily).

Submitted 29 January 2024
Accepted 8 July 2024
Published 14 August 2024
10.1126/sciadv.ado3258